Intelligent Search Optimized Edge Potential Function (EPF) Approach to Synthetic Aperture Radar (SAR) Scene Matching

Yifei Wang
Intelligent Systems Group
Department of Computer Science
University of Bath
Bath, BA2 7AY, United Kingdom
Email: yifei.wang@ieee.org

Jihao Yin
School of Astronautics
Beihang University
Beijing, 100191, China
Email: yjh@buaa.edu.cn

***Abstract*—Research on synthetic aperture radar (SAR) scene matching in the aircraft end-guidance has a significant value for both research and real-world application. The conventional scene matching methods, however, suffer many disadvantages such as heavy computation burden and low convergence rate so that these methods cannot meet the requirement of end-guidance system in terms of fast and real-time data processing. Furthermore, there are complex noises in the SAR image, which also compromise the effectiveness of using the conventional scene matching methods. To address the above issues, in this paper, the intelligent optimization method, Free Search with Adaptive Differential Evolution Exploitation and Quantum-Inspired Exploration, has been introduced to tackle the SAR scene matching problem. We first establish the effective similarity measurement function for target edge feature matching through introducing the edge potential function (EPF) model. Then, a new method, ADEQFS-EPF, has been proposed for SAR scene matching. In ADEQFS-EPF, the previous studied theoretical model, ADEQFS, is combined with EPF model. We also employed three recent proposed evolutionary algorithms to compare against the proposed method on optical and SAR datasets. The experiments based on Matlab simulation have verified the effectiveness of the application of ADEQFS and EPF model to the field of SAR scene matching.**

I. Introduction

High-resolution synthetic aperture radar (SAR) is an active high-resolution microwave remote sensor. From early sixties in the twentieth century, SAR played a significant role in military scouting [1]. A large quantity of available airborne SAR images have changed the conventional view that microwave imaging only has a low quality on spatial resolution. In addition, the full-time using of SAR gives a remarkable impression on the researchers. As an emerging new imaging tool, SAR has an immense influence on the field of precise control and guidance. The research on SAR scene matching in the aircraft end-guidance therefore has a promising future for military application. It also has a significant contribution on further improving the air-strikes correctness and preciseness, fast weakening the enemys combat strength, and effectively obtaining the turning point in the battlefield.

In the SAR scene matching of aircraft end-guidance system, the navigation error is corrected by the combination of current navigation information from GPS, for example, and the most up-to-date information of target position from aided navigation system. The updated position information can be obtained through matching of the SAR real-time image with the reference image that has been pre-uploaded to the system. Therefore, the SAR scene matching method is one of critical techniques in such an aided navigation system, which requires real-time performance, sub-pixel accuracy and high robustness.

It has been shown that the matching performance can be greatly improved by using boundary-based methods [2]. Boundary-based scheme is therefore considered as an effective way to simultaneously obtain both the position errors and yawing errors. Generally, there are two critical steps involved in boundary-based matching approach: contour extraction and similarity measuring [3]. However, the SAR image, even the high-resolution image after filtering and processing, is greatly different from the optical image. Targets in SAR images are quite dimmer and their details are very vague. In addition, the SAR images usually contain many severe speckle noises compared to common optical images [4], [5]. Therefore, many traditional feature extraction and similarity measuring approaches become invalid or less effective and they cannot meet the requirement for end-guidance system in terms of fast and real-time data processing.

Recently, the Edge Potential Function (EPF) model has been proposed and developed by Minh-Son et al to measure the similarity between two images that need to be matched [6]. This conception is derived from the physics of electricity. It is used to build the desired model which includes edge position, strength and continuity in a powerful representation, called edge map. The edge map can describe the attraction generated by edge structures contained in an image over similar curves. Such a novel approach has been proved its feasibility and reliability in complex environment [6]–[8]. The EPF model is therefore expected to deal with scene matching problem in SAR images.

It is yet another important step that we need a powerful searching technique in order to apply boundary-based matching approach to SAR aided navigation system. Given that the attraction field associated to the EPF model is a complex and multi-modal function, the searching algorithm should be highly robust. Evolutionary algorithms are therefore suitable to complete the task as these population-based algorithms are popular search techniques for solving global optimization problems with unknown structure to the objective function. Many computational evolutionary algorithms are now used to solve real-world industrial optimization problems [9]–[13]. The Free Search with Adaptive Differential Evolution

Exploitation and Quantum-Inspired Exploration (ADEQFS) is a newly population-based optimization algorithm proposed by Yin et al in 2012 [14]. The ADEQFS algorithm, derived from Free Search [15], [16], can be easy to implement with high computation efficiency and rapid convergence.

In this paper, we focused on applying the novel similarity measuring approach and powerful searching technique to the SAR scene matching system. To be specific, the ADEQFS optimized EPF approach has been proposed and developed to deal with the scene matching for SAR images. We first established the effective fitness function through introducing the EPF model. Then, a new method, ADEQFS-EPF, was proposed where the previous studied theoretical model, ADEQFS, is combined with EPF model. In order to study the effectiveness of the proposed approach, we also employed other three advanced evolutionary algorithms PS^{2}O [17], JADE [18], [19] and ABC [8], [20], developed from particle swarm optimization, differential evolution, and artificial bee colony, respectively, to compare against the proposed algorithm on both normal optical and SAR datasets. The visual and quantitative results highlight the benefits of the proposed novel approach and its potential to be used in the SAR aided navigation system.

The remainder of the paper is organized as follows. In Section II, some key techniques such as affine transformation, EPF model and ADEQFS algorithm are reviewed. The proposed approach, ADEQFS-EPF, is described in details in Section III. Experiments, results interpretation and analysis are presented in Section IV. Finally, Section V gives a concise summary of our work.

II. Related Work

A. Affine Transformation

In the SAR scene matching aided navigation system, the detected images are subject to geometric distortion introduced by perspective irregularities wherein the position of the SAR imaging sensor with respect to the scene alters the apparent dimensions of the scene geometry. Using an affine transformation to a uniformly distorted image can correct for a range of perspective distortions by transforming the measurements from the ideal coordinates to those actually used.

An affine transformation [21] is an important class of linear 2-D geometric transformations which maps the current location (x, y) in the original image to the new position (x', y') in the output image by applying a linear combination of translation, rotation and scaling operations. The affine transformation from a reference image point (x_i, y_i) to a real-time image point (x'_i, y'_i) can be written as:

$$\begin{bmatrix} x'_i \\ y'_i \end{bmatrix} = k \cdot \begin{bmatrix} \cos(\theta) & \sin(\theta) \\ -\sin(\theta) & \cos(\theta) \end{bmatrix} \cdot \begin{bmatrix} x_i \\ y_i \end{bmatrix} + \begin{bmatrix} t_x \\ t_y \end{bmatrix}, \quad (1)$$

where the model translation is $[t_x, t_y]^T$ and the affine rotation and scaling are represented by θ and k, respectively.

In this paper, the ADEQFS algorithm is employed to find the optimal parameters (t_x, t_y, θ, k) of affine transformation for the sketch template to match up with the targets in the scene images.

B. EPF Model

The Edge Potential Function (EPF) model derived from the potential generated by charged particles was firstly developed by Minh-Son et al [6]. The EPF model is tailored to the context of image matching, where it can be used to attract a template of the searched object or a sketch drawn by a user in the position where a similar shape is present in the image.

In complete analogy with the charged particles, the ith edge point in the image at coordinate (x_i, y_i) can be assumed to be equivalent to a point charge $Q_{eq}(x_i, y_i)$, contributing to the potential of all image pixels:

$$EPF(x, y) = \frac{1}{4\pi\varepsilon_{eq}} \sum_i \frac{Q_{eq}(x_i, y_i)}{\sqrt{(x - x_i)^2 + (y - y_i)^2}}, \quad (2)$$

where ε_{eq} is a constant measuring the equivalent permittivity of image background, taking into account the extent of the attraction of each edge point. It should be noted that ε_{eq} influences the spread of the potential function making it more steep or smooth depending on its magnitude. In order to simplify the calculations and improve the robustness of shape-matching in noisy environments, we adopted the Binary EPF, where all edge points are modelled as equal charges, i.e., $Q_{eq} = Q_{eq}(x_i, y_i)$, as a constant.

To complete the model, the object template that needs to be matched with the edge map can be considered as a test object in the equivalent edge potential field generated from the image. Consequently, the template is expected to be attracted by a set of equivalent charged points that maximizes the potential along the edge. In this way, the higher the similarity between the object template and searched target in the image, the higher the total attraction engendered by the edge field. Therefore, EPF model can be ideally used as the similarity measure for SAR scene matching task because it implicitly includes many important features such as edge position, strength, and continuity, in a unique powerful representation of the edge.

C. ADEQFS Algorithm

The recently proposed approach Free Search [15], [16] has introduced the concept of sensibility, allowing the individuals exploring any location in the search space with positive probability. However, such a strategy is difficult to implement because it requires a priori key knowledge that is not clearly defined in existing literature. To address this issue, the authors in [14] proposed a new implementation for the concept model of Free Search. In the proposed algorithm, Free Search with Adaptive Differential Evolution Exploitation and Quantum-Inspired Exploration (ADEQFS), the authors focused on designing a hybrid mutation strategy. Particularly, in the ADEQFS algorithm, all the individuals, called H-animals, are embedded with two types of information: adaptive differential evolution information and quantum-inspired information. H-animals conduct different search behaviours balanced between the exploitation search and the exploration search. Specifically, H-animals start with random locations in the search space. For each H-animal, the location fitness, adaptive differential evolution information and quantum-inspired are evaluated and calculated. Then, H-animal distributes pheromone in an

amount proportional to the amount of the solution found. H-animals' exploration, which is favoured at the beginning, and exploitation, which is preferred at the end, are executed in the search process. Each H-animal's H-sense is generated randomly. Then, each H-animal selects a location with a restricted condition that the pheromone of the current location is better than its sense. During the local search, the H-animal exploits the current location with a small step size by using its adaptive differential evolution information, whereas during the global search, the H-animal explores around the current location with a large step size by using its quantum-inspired information. The H-animal takes H-step after performing either exploitation or exploration processes. Then, the H-animal updates the locations if it finds a better one. At last, the two types of information are updated. The whole process is repeated until a stopping criterion is met. The pseudo code of ADEQFS's procedure can be found in [14].

The ADEQFS algorithm is easy to implement with rapid convergence rate and high computation reliability. In this paper, the matching process was implemented by ADEQFS specifically designed for the task, finding the optimal parameters in the search space (defined in Section II-A), to locate the targets in the edge maps extracted from original images (defined in Section II-B).

III. ADEQFS-EPF Approach to SAR Scene Matching

A. Fitness Function for Scene Matching

To solve SAR scene matching problem, we need first build an appropriate fitness function that can be optimized by ADEQFS algorithm later on. In Section II-B, we can see that when the test template is approaching to the target in the image, the total attraction engendered by the the edge potential field will be maximized. Therefore, the objective function for SAR scene matching problem can be defined as

$$f_{opt}(c_g) = \sum_{n^{(c_g)}=1}^{N^{(c_g)}} \{EPF\,(x_n^{c_g}, y_n^{c_g})\}, \tag{3}$$

where, $c_g = (x_g, y_g, \theta_g, k_g)$ represents the parameter vector of affine transformation, calculated by ADEQFS, i.e., (x_g, y_g), θ_g, k_g are the matched coordinate, rotation parameter and scaling parameter, respectively, found by ADEQFS at g^{th} generation, and $N^{(c_g)}$ represents the total number of pixels along the potential edge.

Given that the ADEQFS algorithm is born to deal with minimized problems, we can simply re-write the Eq(3) as

$$f(c_g) = \frac{1}{1 + \sum\limits_{n^{(c_g)}=1}^{N^{(c_g)}} \left\{EPF\left(x_n^{c_g}, y_n^{c_g}\right)\right\}}. \tag{4}$$

From the above equation, we can clearly see that when $f(c_g)$ gets the minimized value, the total attraction, i.e. Eq(4), will be maximized. We can therefore use Eq(4) as the fitness function that can be minimized by ADEQFS algorithm.

It should be noted that optimal value of $N^{(c_g)}$ is a constant which is related to the target in the image that needs to be matched, that is, there is only one function peak for the total attraction calculated by Eq(4). Therefore, the optimal vale in Eq(4) will not be changed at each iteration. In other words, although $N^{(c_g)}$ which is used calculate the Eq(4) could be different at each iteration due to some missing points in test template after affine transformation, for example. But the fitness function can get the optimal value if and only if the number of points along the edge field is the same or close to $N^{(c_g)}$. Therefore, $N^{(c_g)}$ may be changed in each iteration, but the optimal value of $N^{(c_g)}$ will be unaffected and therefore the optimal value of Eq(4) will not be changed.

B. ADEQFS-EPF Implementation

The details of ADEQFS-EPF are described as below.

Step 1: Data Preprocessing. Load SAR scene matching image, and convert it into grayscale format for further edge detection operation.

Step 2: Edge Extraction. Adopt canny edge extractor to detect the edges of the given image for the sake of obtaining edge potential field of the original image.

Step 3: Edge Potential Field Calculation. Using Eq(2) to calculate the EPF distribution of the original image.

Step 4: ADEQFS Initialization. Set the population size NP, the maximum iteration times G, and the problem dimension $ND = 4$. Create initial population and set $g = 1$.

Step 5: ADEQFS Searching. Load the test template, and use ADEQFS algorithm to search its optimal parameter vector $(x_{opt}, y_{opt}, \theta_{opt}, k_{opt})$ so that it can be matched up with the target after affine transformation with maximum total attraction calculated by Eq(4).

Step 6: Iteration. Repeat the same processes of ***Step 5***, until g has reached to the maximum iteration times G or the optimization criteria.

Step 7: Output. Output the optimal parameter vector of affine transformation. Locate the target in the scene image.

IV. Experiments and Results

In this section, the proposed approach has been tested on both optical and SAR images. We also use three advanced evolutionary algorithms [1] that were proposed recently: PS^{2}O, JADE and ABC proposed in [17], [19] and [8], respectively, to compare against the effectiveness of using ADEQFS in the proposed approach. In this paper: for relatively fair comparison, we set the all the common used parameters to be the same: $\varepsilon_{eq} = 0.01$ and $Q_{eq} = 1$. The search spaces of parameters in affine transformation are: $1 \le x \le row_{\max}$, $1 \le y \le col_{\max}$, where $row_{\max}$ and $col_{\max}$ are the maximum of row and column coordinate in the given image, $0^\circ \le \theta \le 360^\circ$ and $0.1 \le k \le 1.5$, respectively.

[1] The reasons to choose these algorithms are 1) they are representative algorithms proposed recently in trending evolutionary computation sub-branches, and 2) The matching approach based on ABC proposed in [8] is similar to this paper and therefore it can be a good reference.

A. Results and Analysis for Scene Matching on Optical Dataset

In the experiments for scene matching on optical dataset, we set the population size $NP = 20$, the maximum iteration times $G = 100$ and the problem dimension $ND = 4$. For relatively fair comparison, we set and follow the parameter settings suggested in the original paper for the four comparison tests. For PS^{2}O-EPF, we set the number of swarms $n = 5$, $C1$ and $C2$ both 2.05, $C3 = 2.0$, the constriction factor $\chi = 0.729$, and the maximum velocity was set to be 50%. For JADE-EPF and ADEQFS-EPF, we set the parameters, $p = 0.2$ and $c = 0.1$. For ABC-EPF, we set the colony size of the employed bees to be $N_e = NP/2$, the size of unemployed bees to be $N_u = NP/2$ and the largest searching times to be $P_{Limit} = 100$. The original optical image with the size of 237×361 as well as its edge potential distribution map can be seen in Fig. 1.

(a) The original optical image

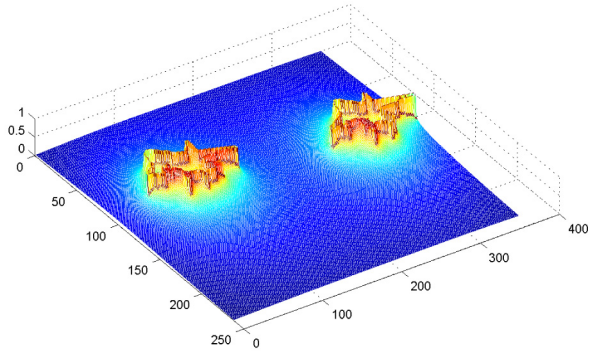

(b) The EPF map

Fig. 1. The original optical image and its edge potential distribution map

In order to test the effectiveness of the proposed approach, we employed the left-side plane in the Fig. 1a as the target that needs to be matched. We first used the canny edge extractor to detect the edges of the left-side plane, and then used $(\theta = 330°, k = 1.25)$ and $(\theta = 30°, k = 0.8)$ as the parameters of affine transformation to get two different test templets as shown in Fig. 2.

In the first experiment, we used the plane test template in Fig. 2a to find the target plane in the original image. For each of four test approaches, we run 5 times independently. The results are summarized in Table I. We also plotted the best

[2]Note: For better visualization, this sketch has been zoomed 2 times bigger than the actual test templates.

(a) Test template 1

(b) Test template 2

Fig. 2. The plane test templates [2]

results, which are bolded in Table I, in 5 runs to visually compare the performance among different approaches as shown in Fig. 3.

(a) PS^{2}O-EPF

(b) JADE-EPF

(c) ABC-EPF

(d) ADEQFS-EPF

Fig. 3. Visual comparison for scene matching using plane test template 1

After a $30°$ rotation, 0.8 times scaling, and a $[72, 40]$ translation, the target can be successfully matched up in the original image, which means that the best geometric parameters are $([72, 40], 30°, 0.8)$. From Table I, we can see that the results obtained by ADEQFS-EPF were very closed to the optimal solution in all 5 independent runs. Although ABC-EPF also achieved relatively acceptable results, its matching accuracy was not as good as ADEQFS-EPF's approach. PS^{2}O-EPF and JADE-EPF were more likely to be trapped in the local optima.

In the second experiment, we used the plane test template in Fig. 2b to find the target plane in the original image. Similar to the first experiment, for each of four test approaches, we run 5 times independently. The results are summarized in Table II. We also plotted the best results, which are bolded in Table II, in 5 runs to visually compare the performance among different approaches as shown in Fig. 4.

After a $330°$ rotation, 1.25 times scaling, and a $[72, 40]$ translation, the target can be successfully matched up in the original image, which means that the best geometric parameters are $([72, 40], 330°, 1.25)$. From Table II, we can see that the results obtained by ADEQFS-EPF were very closed to the optimal solution in all 5 independent runs. Although ABC-EPF found a good solution in the first run, it falsely matched up with the right-side plane in 3^{rd} and 4^{th} runs. PS^{2}O-EPF and JADE-EPF were also wrongly confused the left-side target with the right-side plane.

TABLE I. THE COMPARISON RESULTS OF PLANE MATCHING AMONG FOUR DIFFERENT APPROACHES (OPTIMAL SOLUTION: [72,40], 30°, 0.8)

	1	2	3	4	5
PS^{2}O-EPF	101, 245, 179.49°, 0.90	109, 19, 23.45°, 1.47	**99, 258, 236.15°, 0.61**	62, 179, 37.50°, 1.18	54, 237, 151.88°, 1.22
JADE-EPF	60, 75, 349.75°, 0.70	1, 1, 265.38°, 0.10	20, 52, 264.14°, 0.89	47, 27, 242.07°, 0.95	**68, 38, 233.96°, 0.71**
ABC-EPF	71, 38, 29.65°, 0.83	72, 41, 30.55°, 0.78	**72, 44, 30.62°, 0.69**	77, 37, 210.52°, 0.78	76, 45, 26.86°, 0.75
ADEQFS-EPF	**72, 40, 29.76°, 0.80**	72, 40, 29.82°, 0.80	72, 39, 29.94°, 0.80	72, 39, 29.88°, 0.80	72, 40, 30.39°, 0.79

TABLE II. THE COMPARISON RESULTS OF PLANE MATCHING AMONG FOUR DIFFERENT APPROACHES (OPTIMAL SOLUTION: [72,40], 330°, 1.25)

	1	2	3	4	5
PS^{2}O-EPF	**71, 286, 283.46°, 1.12**	72, 274, 196.99°, 1.19	115, 87, 176.52°, 1.32	104, 51, 111.12°, 1.18	113, 245, 97.29°, 1.01
JADE-EPF	**82, 45, 150.38°, 0.95**	72, 277, 265.44°, 1.01	72, 277, 265.44°, 1.01	97, 53, 154.84°, 0.86	72, 266, 22.27°, 1.09
ABC-EPF	78, 48, 326.44°, 1.10	**72, 42, 331.67°, 1.18**	92, 254, 325.74°, 1.17	86, 244, 328.70°, 1.33	80, 40, 147.60°, 1.06
ADEQFS-EPF	72, 40, 330.04°, 1.26	72, 41, 329.84°, 1.24	72, 41, 330.04°, 1.24	72, 40, 330.04°, 1.23	**72, 40, 329.95°, 1.25**

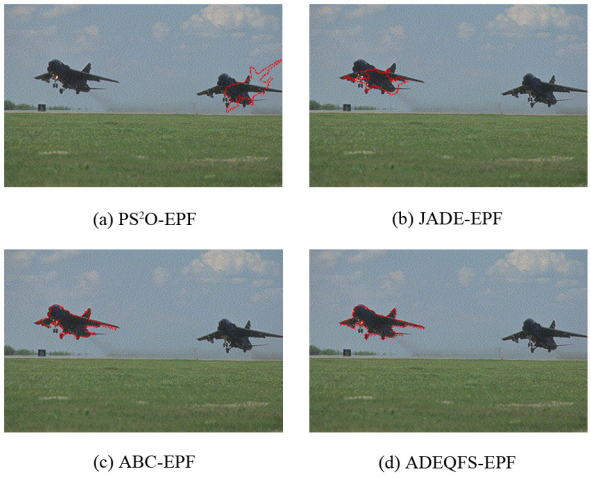

(a) PS^{2}O-EPF (b) JADE-EPF

(c) ABC-EPF (d) ADEQFS-EPF

Fig. 4. Visual comparison for scene matching using plane test template 2

To further test the matching speed and reliability of the proposed approach against other methods, we used the two plane test templates to conduct two additional experiments. For each approach on each of two tests, we executed 100 independent runs. It should be noted that we employed average function evaluations (AFEs) instead of real time to measure the matching speed. This is because all the test approaches have a similar computational burden, and the code has not been optimized. Therefore, it is useless to compare the real searching time. We also used the success rate (SR) of each algorithm to measure the reliability. In both experiments, we set the maximum iteration times $G = 200$. The rest of parameters were set the same as before. The matching precisions of parameters in affine transformation were set: 1 pixel for translation, 1° for rotation and 0.1 for scaling. Therefore, when using the test template in Fig. 1a, the stopping criteria are: $x = 72 \pm 1$, $y = 40 \pm 1$, $\theta = 30° \pm 1°$ and $k = 0.8 \pm 0.1$, whereas the criteria: $x = 72 \pm 1$, $y = 40 \pm 1$, $\theta = 330° \pm 1°$ and $k = 1.25 \pm 0.1$ are for the test template in Fig. 1b. In both experiments, if the test approach failed to find the optimal solution, the experiment will be stopped at 200^{th} iteration. The results are summarized in Table III and Table IV, respectively.

As can be seen in Table III and Table IV, the proposed ADEQFS-EPF has strictly high matching speed and reliability. Although ABC-EPF approach can find the optimal solution within the given maximum iterations, it was failed in some cases. It should be noted that the error precision was set to be relatively high in both experiments, Therefore, the PS2^{2}O-EPF and JADE-EPF approaches cannot achieve a good performance.

TABLE III. THE MATCHING SPEED AND RELIABILITY COMPARISON RESULTS ($x = 72 \pm 1$, $y = 40 \pm 1$, $\theta = 30° \pm 1°$, $k = 0.8 \pm 0.1$)

	PS^{2}O-EPF	JADE-EPF	ABC-EPF	ADEQFS-EPF
SR	0%	0%	46%	100%
AFEs	–	–	151	59

TABLE IV. THE MATCHING SPEED AND RELIABILITY COMPARISON RESULTS ($x = 72 \pm 1$, $y = 40 \pm 1$, $\theta = 330° \pm 1°$, $k = 1.25 \pm 0.1$)

	PS^{2}O-EPF	JADE-EPF	ABC-EPF	ADEQFS-EPF
SR	0%	0%	51%	100%
AFEs	–	–	148	83

B. Results and Analysis for Scene Matching on SAR Dataset

In this section, we conducted two experiments on SAR dataset provided by Sandia National Laboratories. In the first experiment, we used a sub-region SAR image (1-m resolution) of size 166×427 in Washington, D.C. The data was obtained by a Ku-Band (15 GHz) SAR carried by the Sandia Twin Otter aircraft. The used sub-region SAR image as well as its edge potential distribution map can be seen in Fig. 5. In this sub-region image, the target that needs to be matched is the Pentagon. The target sketch, which was used as the test template, can be seen in Fig. 6.

(a) The original SAR image

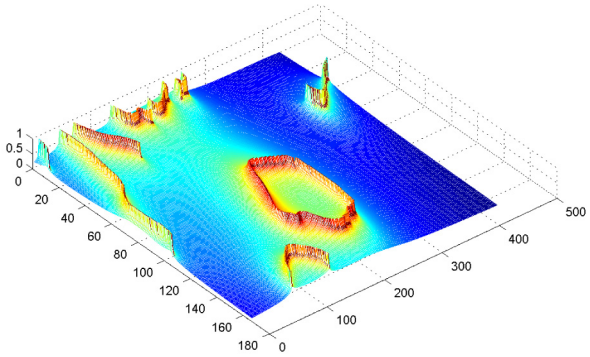

(b) The EPF map

Fig. 5. The sub-region SAR image in Washington, D.C. and its edge potential distribution map

Fig. 6. The test template of Pentagon sketch [3]

In this experiment, we set the population size $NP = 30$, the maximum iteration times $G = 50$ and the problem dimension $ND = 4$. All other parameters were set as same as in Section IV-A. For each of four test approaches, we run 5 times independently. The results are summarized in Table V. We also plotted the best results, which are bolded in Table V, in 5 runs to visually compare the performance among different approaches as shown in Fig. 7. It should be noted that the used Pentagon test template was a manual sketch. Therefore, there is no theoretical optimal solution so that we can conduct further experiments on testing matching speed and reliability.

From Table V and the visual comparison in Fig. 7, we can see that ADEQFS-EPF approach achieved the best overall performance in all 5 independent runs. The PS^{2}O-EPF, ABC-EPF and JADE-EPF also obtained relatively good results, but they were still inferior than ADEQFS-EPF and were easily trapped in the local optima. It should be noted that because the shape of sketch template is similar to a perfect pentagon, it is possible that the visual results are similar but differ greatly in numerical results. In terms of the accuracy of ADEQFS-EPF matching results, they are not as perfect as we expect. This is mainly due to the inaccuracy of edge detection when using Canny edge extractor.

(a) PS^{2}O-EPF

(b) JADE-EPF

(c) ABC-EPF

(d) ADEQFS-EPF

Fig. 7. Visual comparison for scene matching using pentagon test template

In the second experiment, we used a sub-region SAR image (1-m resolution) of size 302×351 in Hangers at Kirtland AFB, Albuquerque, New Mexico. The data was obtained by an X-Band (10 GHz) SAR carried by the Sandia Twin Otter Aircraft. The used sub-region SAR image as well as its edge potential distribution map can be seen in the Fig. 8. In this sub-region image, the target that needs to be matched is a building. The target sketch, which was used as the test template, can be seen in Fig. 9.

In this experiment, we set the population size $NP = 50$, the maximum iteration times $G = 100$ and the problem dimension $ND = 4$. All other parameters were set as same as in Section IV-A. For each of four test approaches, we run 5 times independently. The results are summarized in Table VI. We also plotted the best results, which are bolded in Table VI, in 5 runs to visually compare the performance among different approaches as shown in Fig. 10. It should be noted that the used building test template was also a manual sketch. Therefore, similarly we cannot test the matching speed and reliability of ADEQFS against other approaches.

From Table VI and the visual comparison in Fig. 10, we can clearly see that the results achieved by ADEQFS-EPF approach outperformed all other tested approaches. Although the PS^{2}O-EPF, ABC-EPF and JADE-EPF can locate the position that was very close to the target, the accuracy was not as good as

[3]Note: For better visualization, this sketch has been zoomed 2 times bigger than the actual sketch template.

TABLE V. THE COMPARISON RESULTS OF THE PENTAGON MATCHING AMONG FOUR DIFFERENT APPROACHES

	1	2	3	4	5
PS^{2}O-EPF	94, 200, 4.28°, 0.57	9, 187, 78.74°, 1.39	**74, 141, 119.76°, 0.90**	55, 196, 165.46°, 0.57	62, 182, 33.98°, 0.79
JADE-EPF	82, 144, 295.99°, 0.81	9, 135, 201.51°, 1.42	**77, 175, 334.16°, 0.81**	34, 132, 200.69°, 1.12	55, 156, 278.59°, 1.06
ABC-EPF	72, 173, 59.89°, 0.84	74, 172, 118.80°, 0.80	**72, 169, 104.16°, 0.84**	79, 158, 72.42°, 0.83	73, 160, 96.32°, 0.96
ADEQFS-EPF	77, 164, 297.01°, 0.85	78, 162, 302.44°, 0.79	75, 163, 305.12°, 0.85	77, 166, 309.78°, 0.81	**78, 164, 299.86°, 0.83**

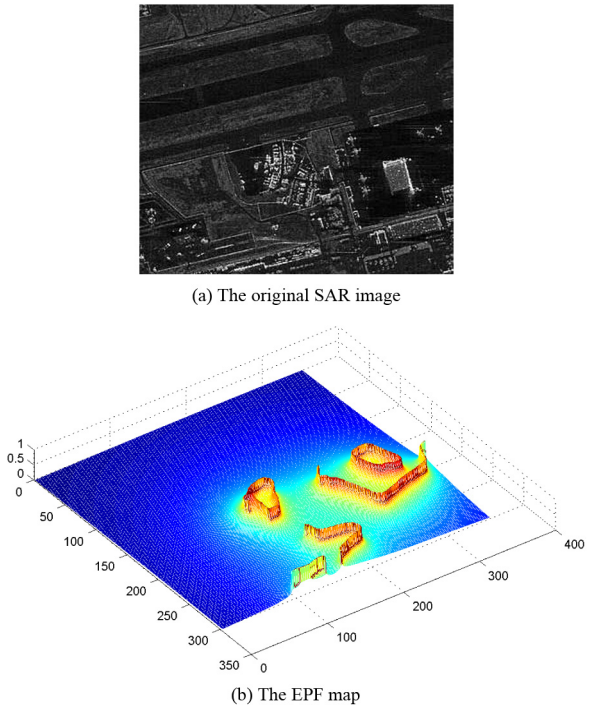

(a) The original SAR image

(b) The EPF map

Fig. 8. The sub-region SAR image in Hangers and its edge potential distribution map

Fig. 9. The test template of building sketch [4]

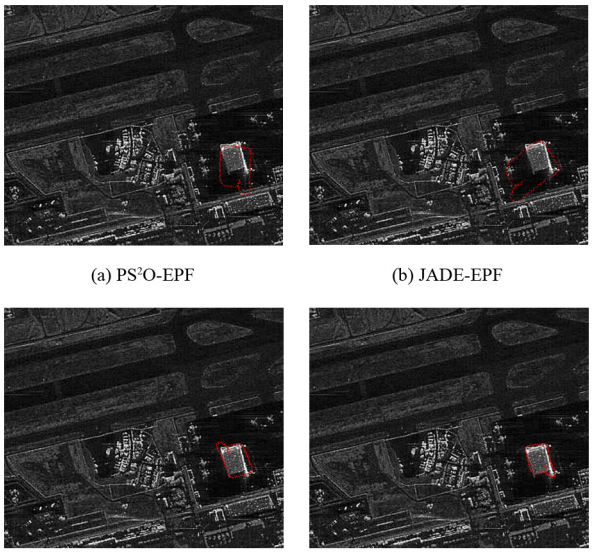

(a) PS^{2}O-EPF (b) JADE-EPF

(c) ABC-EPF (d) ADEQFS-EPF

Fig. 10. Visual comparison for scene matching using building test template

compared with the proposed ADEQFS-EPF approach, meaning that they were more likely to be trapped in the local optima and ADEQFS-EPF achieved the best overall performance.

V. CONCLUSIONS

A new approach of SAR scene matching using ADEQFS optimized edge potential function has been described and assessed. Specifically, by introducing the EPF model, the target matching problem was converged into an optimal issue that can be solved by a newly proposed ADEQFS algorithm. The main advantage of using EPF model is that it enables the proposed approach to exploit the joint effect of single edge points in complex structures more efficiently, achieving a better global matching. The edge potential can be easily calculated from an edge map extracted from the image, and represents a sort of attraction field in analogy with the field generated by a charged element. Then, the problem can be restated to find the optimal parameters (position, rotation and scaling factor) that maximize the overlapping between sketch and target. Finally, the ADEQFS algorithm can be employed to find these optimal parameters in the given search space. In order to test the performance of proposed approach, we conducted two groups of experiments on both optical images and SAR images. We also use three advanced evolutionary algorithms PS^{2}O, JADE and ABC to compare against the effectiveness of using ADEQFS in the proposed approach. The numerical and visual results highlight the matching speed and computation reliability of using proposed ADEQFS-EPF approach.

Compared with optical images, one of salient features in SAR images is that it contains the heavy multiplicative noise, which significantly decares the feature extraction performance. The benefits of using the proposed ADEQFS-EPF approach in SAR scene matching system are presented in two ways: 1) Fast matching speed. The proposed ADEQFS-EPF approach is

TABLE VI. THE COMPARISON RESULTS OF BUILDING MATCHING AMONG FOUR DIFFERENT APPROACHES

	1	2	3	4	5
PS^{2}O-EPF	189, 252, 223.60°, 1.17	**176, 270, 360.00°, 1.16**	180, 223, 321.37°, 1.46	188, 273, 252.53°, 1.14	197, 246, 242.13°, 1.30
JADE-EPF	162, 132, 313.24°, 0.75	170, 246, 51.05°, 1.41	184, 261, 158.70°, 1.11	**168, 266, 155.46°, 0.92**	198, 250, 253.33°, 1.06
ABC-EPF	189, 243, 253.10°, 1.28	170, 264, 146.58°, 0.93	191, 246, 249.72°, 1.20	**168, 266, 155.46°, 0.92**	169, 265, 152.53°, 0.90
ADEQFS-EPF	169, 270, 336.60°, 0.88	169, 272, 339.87°, 0.84	170, 271, 339.20°, 0.89	169, 272, 340.18°, 0.85	**170, 271, 343.18°, 0.84**

designed for the SAR scene matching aided navigation system. Therefore, the traditional matching techniques based on the image sequential scanning are not feasible as they cannot meet the requirement for end-guidance system in terms of fast and real-time data processing. 2) High adaptability. The proposed ADEQFS-EPF approach uses the EPF model, which is suitable to be applied to matching problem in complex environment, to measure the similarity between the test template and the target in the scene image. Therefore, the EPF model provides the proposed approach with high matching accuracy and robustness in presence of complex noise in SAR images.

ACKNOWLEDGMENTS

This work received the support from the National High Technology Research and Development Program of China ("863" Program) and National Natural Science Foundation of China and Chinese Academy of Sciences Joint Fund of Astronomy (Grant U1331108). The authors also wish to thank anonymous reviewers who gave valuable suggestions that have helped to improve the quality of the manuscript.

REFERENCES

[1] J. Bevington and C. Marttila, "Precision aided inertial navigation using sar and digital map data," in *Position Location and Navigation Symposium, 1990. Record. The 1990's - A Decade of Excellence in the Navigation Sciences. IEEE PLANS '90., IEEE*, 1990, pp. 490–496.

[2] S. Belongie, J. Malik, and J. Puzicha, "Shape matching and object recognition using shape contexts," *Pattern Analysis and Machine Intelligence, IEEE Transactions on*, vol. 24, no. 4, pp. 509–522, 2002.

[3] L. Olsen, F. F. Samavati, M. C. Sousa, and J. A. Jorge, "Sketch-based modeling: A survey," *Computers and Graphics*, vol. 33, no. 1, pp. 85–103, 2009.

[4] X. Hua, L. E. Pierce, and F. T. Ulaby, "Sar speckle reduction using wavelet denoising and markov random field modeling," *Geoscience and Remote Sensing, IEEE Transactions on*, vol. 40, no. 10, pp. 2196–2212, 2002.

[5] S. Yongwei and D. E. Alsdorf, "Automated georeferencing and orthorectification of amazon basin-wide sar mosaics using srtm dem data," *Geoscience and Remote Sensing, IEEE Transactions on*, vol. 43, no. 8, pp. 1929–1940, 2005.

[6] D. Minh-Son, F. G. B. De Natale, and A. Massa, "Edge potential functions (epf) and genetic algorithms (ga) for edge-based matching of visual objects," *Multimedia, IEEE Transactions on*, vol. 9, no. 1, pp. 120–135, 2007.

[7] H. Li, H.-B. Duan, and X.-Y. Zhang, "A novel image template matching based on particle filtering optimization," *Pattern Recognition Letters*, vol. 31, no. 13, pp. 1825–1832, 2010.

[8] C. Xu and H. Duan, "Artificial bee colony (abc) optimized edge potential function (epf) approach to target recognition for low-altitude aircraft," *Pattern Recognition Letters*, vol. 31, no. 13, pp. 1759–1772, 2010.

[4]Note: For better visualization, this sketch has been zoomed 3 times bigger than the actual sketch template.

[9] A. Ponsich and C. A. C. Coello, "Differential evolution performances for the solution of mixed-integer constrained process engineering problems," *Applied Soft Computing*, vol. 11, no. 1, pp. 399–409, 2011.

[10] R. Precup, R. David, E. M. Petriu, S. Preitl, and M. Radac, "Novel adaptive gravitational search algorithm for fuzzy controlled servo systems," *Industrial Informatics, IEEE Transactions on*, vol. 8, no. 4, pp. 791–800, 2012.

[11] J. Yin, Y. Wang, and J. Hu, "A new dimensionality reduction algorithm for hyperspectral image using evolutionary strategy," *Industrial Informatics, IEEE Transactions on*, vol. 8, no. 4, pp. 935–943, Nov 2012.

[12] M. Z. Ali, K. Alkhatib, and Y. Tashtoush, "Cultural algorithms: Emerging social structures for the solution of complex optimization problems," *International Journal of Artificial Intelligence*, vol. 11, no. A13, pp. 20–42, Oct. 2013.

[13] S. K. Saha, S. P. Ghoshal, R. Kar, and D. Mandal, "Cat swarm optimization algorithm for optimal linear phase fir filter design," *ISA Transactions*, vol. 52, no. 6, pp. 781–794, 2013.

[14] J. Yin, Y. Wang, and J. Hu, "Free search with adaptive differential evolution exploitation and quantum-inspired exploration," *Journal of Network and Computer Applications*, vol. 35, no. 3, pp. 1035–1051, 2012.

[15] K. Penev and G. Littlefair, "Free search — a comparative analysis," *Information Sciences*, vol. 172, no. 12, pp. 173–193, 2005.

[16] K. Penev, "Free search — a model of adaptive intelligence," in *Adaptive and Intelligent Systems, 2009. ICAIS '09. International Conference on*, 2009, pp. 92–97.

[17] H. Chen, Y. Zhu, K. Hu, and T. Ku, "Rfid network planning using a multi-swarm optimizer," *Journal of Network and Computer Applications*, vol. 34, no. 3, pp. 888–901, 2011.

[18] J. Zhang and A. Sanderson, "Jade: Self-adaptive differential evolution with fast and reliable convergence performance," in *Evolutionary Computation, 2007. CEC 2007. IEEE Congress on*, 2007, pp. 2251–2258.

[19] Z. Jingqiao and A. C. Sanderson, "Jade: Adaptive differential evolution with optional external archive," *Evolutionary Computation, IEEE Transactions on*, vol. 13, no. 5, pp. 945–958, 2009.

[20] D. Karaboga and B. Basturk, "A powerful and efficient algorithm for numerical function optimization: artificial bee colony (abc) algorithm," *Journal of Global Optimization*, vol. 39, no. 3, pp. 459–471, 2007.

[21] Y. Lamdan, J. T. Schwartz, and H. Wolfson, "Object recognition by affine invariant matching," in *Computer Vision and Pattern Recognition, 1988. Proceedings CVPR '88., Computer Society Conference on*, 1988, pp. 335–344.